

Thermoelectric Properties of Sintered FeSi<sub>2</sub> with Microstructural Modification

Michitaka OHTAKI, Daisuke OGURA, Koichi EGUCHI, and Hiromichi ARAI\*

Department of Materials Science and Technology,  
Graduate School of Engineering Sciences, Kyushu University,  
6-1 Kasuga-koen, Kasuga, Fukuoka 816

Partial substitution of Cu, Zn, Nb, Ag, Sb, and In for Fe in FeSi<sub>2</sub> significantly varied the structure of the sintered samples. The thermoelectric power increased with decreasing relative density of the samples, while the electrical conductivity decreased at the same time. However, microstructural modification by increasing the size of the particles composing the samples improved the thermoelectric figure of merit through increase in the thermoelectric power and decrease in the thermal conductivity without affecting the electrical conductivity.

Temperature gradient in a semiconducting solid generates the large thermoelectromotive force by the Seebeck effect. Thermoelectric properties of materials composing an element to generate the electric power employing the Seebeck effect are the key to practical use, since the energy conversion efficiency of the thermoelectric power generation is governed by the thermoelectric figure of merit  $Z = S^2\sigma/\kappa$ , or roughly by the power factor  $S^2\sigma$ , of the materials, where  $S$ ,  $\sigma$ , and  $\kappa$  are the Seebeck coefficient, the electrical and thermal conductivities, respectively.

Iron disilicide (FeSi<sub>2</sub>) is one of the most promising materials for the high-temperature thermoelectric power generation because of its rather large values of  $Z$  at high temperatures, high durability to high-temperature operation in air, and low cost and good availability of the raw materials. The thermoelectric elements made of FeSi<sub>2</sub> for practical use are usually fabricated by sintering the powder compacts of the  $n$ - and  $p$ -type FeSi<sub>2</sub>. Although the semiconducting nature and the doping effect of additives such as Al, Mn, and Co have been extensively studied on bulk bodies<sup>1-5)</sup> and thin films<sup>6-10)</sup> of FeSi<sub>2</sub>, the information about the influence of the structural variation on the thermoelectric properties of the sintered bodies is apparently scarce. The present paper describes that the structural variation of sintered FeSi<sub>2</sub> caused by partial substitution for Fe significantly influences their thermoelectric properties. Moreover, a series of the sintered samples with distinctly different microstructures reveals that the microstructural modification can improve the thermoelectric properties by increasing the thermoelectric power without changing the electrical conductivity.

Sintered samples of FeSi<sub>2</sub> and its partially substituted derivatives were prepared from mixtures of the elements (>99.9%) weighed proportional to their nominal compositions. The mixture was melted at 1250 °C for 3 h *in vacuo*, and then cooled slowly. An ingot thus obtained was pulverized and pressed into a pellet, then sintered at 1150 °C for 3 h *in vacuo* and subsequently annealed at 840 °C in air for 50 h. The annealing procedure is to achieve the phase transition to FeSi<sub>2</sub> ( $\beta$  phase) which is semiconducting and responsible for the large

thermoelectric power.<sup>1,5)</sup> Powder X-ray diffraction (XRD) measurement indicated that all the samples consist of single phase of  $\text{FeSi}_2$  with a slight amount of  $\text{FeSi}$ , and no other impurities were detected. Changes in the XRD peak intensity confirmed that the phase transition to the  $\beta$  phase was complete after 20 h of the annealing.

Effects of the compositional deviation of  $\text{FeSi}_2$  were first examined for the samples at nominal compositions of  $\text{FeSi}_{2+x}$  in which  $x$  was 0 to 0.15, since a slight excess of Si has been reported to improve the thermoelectric properties.<sup>8)</sup> All the samples were  $n$ -type up to 500 °C, and the maximum value of the thermoelectric power in its temperature dependence was the largest at  $x=0.10$ . However, the compositional deviation within the range examined made almost no change in the electrical conductivity. The Seebeck coefficient of  $\text{Fe}_{0.97}\text{M}_{0.03}\text{Si}_{2.1}$  ( $\text{M} = \text{Fe}, \text{Cu}, \text{Sb}, \text{Nb}, \text{Zn}, \text{Ag}, \text{In}$ ) are presented in Fig. 1. The thermoelectric power of the substituted samples fairly differs at the lower temperatures, showing particularly small values for the Sb- and Cu-substitution. Nevertheless, all the samples are  $n$ -type and behave similar to non-substituted one ( $\text{M}=\text{Fe}$ ), exhibiting no apparent doping effect as is the case with Mn-<sup>4,5,9)</sup> and Co-doping<sup>1,9,10)</sup> in which the change of the conduction type and the difference in the behavior of  $S$  are obvious. The doping effect of Sb and Cu therefore appears to be insignificant. In fact, the cross-sectional observation on a JEOL-T330A scanning electron microscope (SEM) revealed that the Sb- and Cu-substituted samples have markedly dense structures compared with that of the non-substituted one. The relative density determined by Archimedes' method were as high as 91 and 93% for Sb and Cu, respectively, whereas those for all others were at around 75%. This densification could be attributed to the fact that addition of Sb to Fe, as well as Cu to Si, forms the phases with lower melting points.<sup>11)</sup> Accordingly, the electrical conductivity of the Sb- and Cu-substituted samples at room temperature was apparently high.

Figure 2 depicts that the values of  $S$  and  $\sigma$  of the substituted samples correlate well with the relative density. An increase in  $\sigma$  with increasing relative density can simply be attributed to an increase in the effective cross section area of the samples. Although decrease in  $S$  with increasing  $\sigma$  is often observed and can be

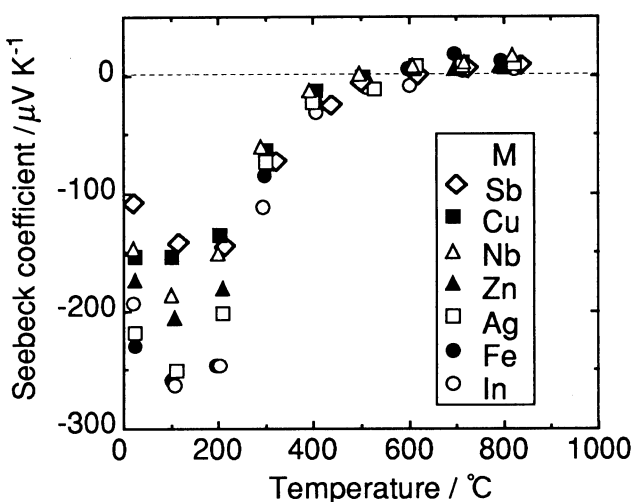


Fig. 1. Temperature dependence of the Seebeck coefficient of  $\text{Fe}_{0.97}\text{M}_{0.03}\text{Si}_{2.1}$ .

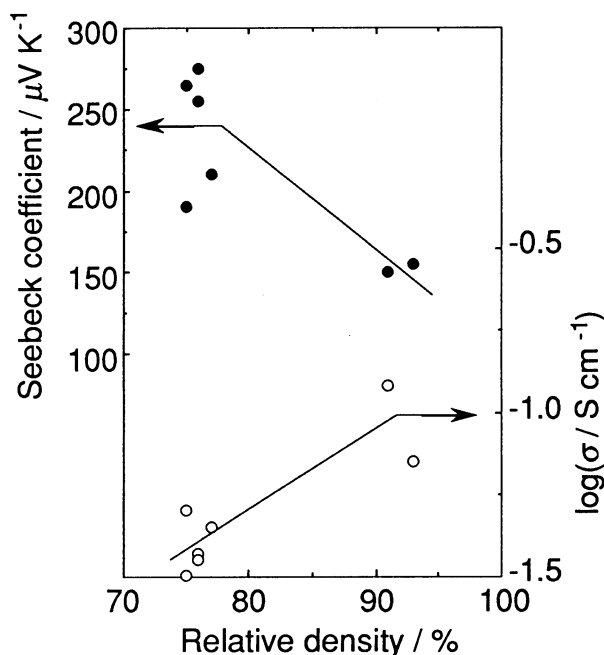


Fig. 2. The relationship between the thermoelectric properties and the relative density of sintered  $\text{Fe}_{0.97}\text{M}_{0.03}\text{Si}_{2.1}$ . ●, The maximum absolute values of the Seebeck coefficient; ○, The electrical conductivity at room temperature.

explained theoretically at least for monocrystalline solids, such explanation will not always hold for the polycrystalline solids as in this study. The reciprocal decrease in  $S$  versus  $\sigma$  seen in Fig. 2 therefore cannot be explained completely by the difference in the relative density. Furthermore, such reciprocal tendency is undesirable for improvement in the thermoelectric performance.

We have therefore intended to examine the effects of the microstructure separately from those of the density. An ingot obtained by melting the stoichiometric amounts of elemental Fe and Si was pulverized to the powder with an alumina mortar (Powder I). The diameters of the major particles in the powder were 100-200  $\mu\text{m}$  determined with SEM. A portion of Powder I was further pulverized with a nylon-lined ball mill, and thereby another powder with the particle size smaller than 50  $\mu\text{m}$  was obtained (Powder II). Three sintered samples were prepared from Powders I, II, and a mixture of an equal amount of Powders I and II, respectively. As seen in Fig. 3, SEM observation revealed that they have definitely different microstructures reflecting the particle size of the starting powders. All three samples, however, have almost the same relative density of *ca.* 75%. The XRD and the SEM/EDX analysis confirmed that the phases and the chemical compositions of these samples are identical, not only in their bulk but also in the particles. Thus, the inhomogeneity of the composition of these samples, or the possibility of any contamination or chemical transformation, *e.g.* the mechanical alloying during the intensive pulverization, has been ruled out.

Nevertheless, the  $S$  values of the sintered samples showed obvious differences as presented in Fig. 4. The thermoelectric power was considerably larger for the samples prepared from the larger particles, in order of Powder I > I+II > II, while the  $\sigma$  values were almost the same, *ca.* 1.0 and -1.5 in  $\log\sigma$  at 500  $^{\circ}\text{C}$  and room temperature, respectively. Consequently, the power factor  $S^2\sigma$  became the largest for the sample prepared from Powder I. Since the improvement in  $S$  is unlikely to be a physical consequence of the difference in the particle diameter,

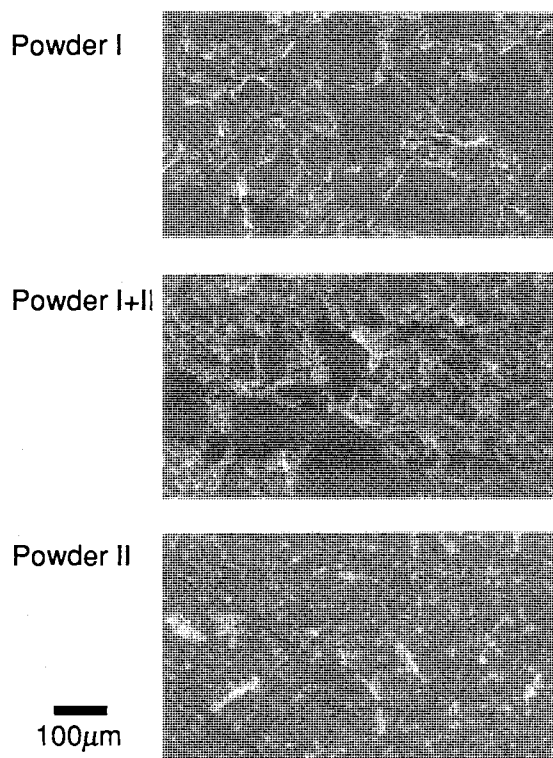


Fig. 3. Scanning electron micrographs of sintered  $\text{FeSi}_2$  prepared from the powders with the different particle sizes.

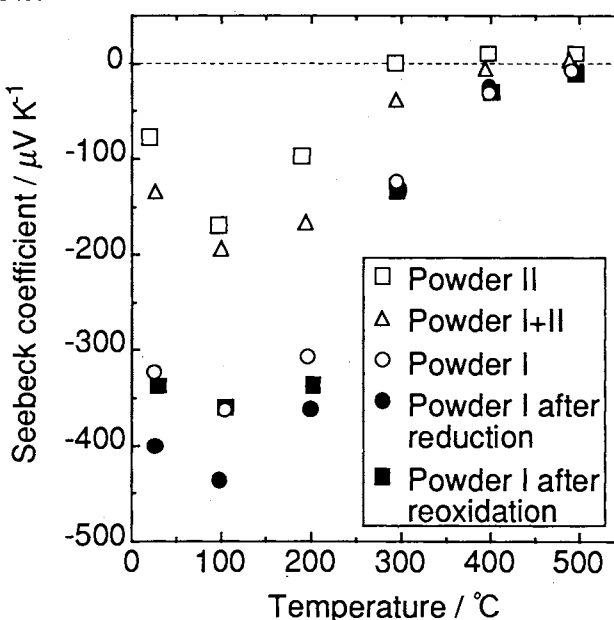


Fig. 4. Temperature dependence of the Seebeck coefficient of sintered  $\text{FeSi}_2$  prepared from the powders with the different particle sizes. Filled symbols denote the values after the post treatments at 800  $^{\circ}\text{C}$ .

we have examined the sintered samples by X-ray photoelectron spectroscopy (XPS). As expected from the information on the transition metal silicides as refractory materials,<sup>12)</sup> an oxide layer mainly consists of SiO<sub>2</sub> was found on the surface, probably resulted from the annealing procedure at 840 °C in air. It is noteworthy that a reductive post treatment in hydrogen at 800 °C for the samples from Powder I further improved *S* as shown with the filled circles in Fig. 4. Moreover, subsequent oxidation treatment in air at the same temperature canceled the effect of the reductive treatment reversibly, putting back the *S* values to those almost the same as the initial values right after the annealing procedure in air. The similar behavior of *S* was also observed for the sample from Powder II, but the extent of the improvement in *S* was larger than that for Powder I. On the other hand, the  $\sigma$  values of both samples showed almost no change during these reduction and oxidation treatments. In addition, neither *S* nor  $\sigma$  varied by the heat treatment in air of the same duration and temperature. These facts strongly suggest that the surface oxide layer of the sintered FeSi<sub>2</sub> decreases *S* without affecting  $\sigma$ . The larger thermoelectric power of the samples with larger particles is probably due to the smaller surface areas. It should also be noted that the thermal conductivity  $\kappa$  of the sample from Powder I was as low as 7.9 and 3.2 W/mK at room temperature and 700 °C, respectively, and lower than that of the sample from the smaller particles, Powder II. The thermoelectric figure of merit,  $S^2\sigma/\kappa$ , consequently attained the maximum value of  $0.3 \times 10^{-4} \text{ K}^{-1}$  at 500–600 °C on the sample from the largest particles, Powder I, with 3% of Mn doping.

In conclusion, the structural changes caused by the partial substitution for Fe accompanied significant variation in the relative density of the sintered FeSi<sub>2</sub>, and both *S* and  $\sigma$  varied in a fairly reciprocal way with the change in the relative density. Nevertheless, the changes in the particle size of the powders composing the sintered samples led to the microstructural modification without changing the relative density. Since the reductive post treatment of the sintered FeSi<sub>2</sub> resulted in an improvement in the thermoelectric power retaining the  $\sigma$  values unchanged, the surface oxide layer should be responsible for the change in *S* observed on these post treatments. The microstructural modification with the increase in the particle size markedly improved the thermoelectric figure of merit of the sintered FeSi<sub>2</sub> through increase in the thermoelectric power and decrease in the thermal conductivity without affecting the electrical conductivity.

## References

- 1) U. Birkholz and J. Schelm, *Phys. Status Solidi*, **27**, 413 (1968).
- 2) U. Birkholz and J. Schelm, *Phys. Status Solidi*, **34**, K177 (1969).
- 3) H. P. Geserich, S. K. Sharma and W. A. Theiner, *Philos. Mag.*, **27**, 1001 (1973).
- 4) I. Nishida, *Phys. Rev. B*, **7**, 2710 (1973).
- 5) T. Kojima, *Phys. Status Solidi (A)*, **111**, 233 (1989).
- 6) T. Lucinski and J. Baszynski, *Phys. Status Solidi (A)*, **84**, 607 (1984).
- 7) M. C. Bost and J. E. Mahan, *J. Appl. Phys.*, **58**, 2696 (1985).
- 8) M. Komabayashi, K.-i. Hijikata and S. Ido, *Jpn. J. Appl. Phys.*, **29**, 1118 (1990).
- 9) M. Komabayashi, K.-i. Hijikata and S. Ido, *Jpn. J. Appl. Phys.*, **30**, 331 (1991).
- 10) M. Komabayashi and S. Ido, *J. Ceram. Soc. Jpn.*, **100**, 22 (1992).
- 11) "Binary Alloy Phase Diagrams," ed by T. B. Massalski, J. L. Murray, L. H. Bennett and H. Baker, American Society for Metals, Metals Park (1986).
- 12) A. W. Searcy, *J. Am. Ceram. Soc.*, **40**, 431 (1957).

(Received March 24, 1993)